ROTORDYNAMIC TESTS OF A FLEXIBLE ROTOR ON FLEXURE PIVOT JOURNAL BEARINGS AND STABILITY CORRELATION WITH FREQUENCY DEPENDENT CHARACTERISTICS

by

Brian C. Pettinato

Development Engineer

and

Pranabesh De Choudhury

Senior Consulting Engineer

Elliott Company

Jeannette, Pennsylvania

Brian Pettinato is a Development Engineer at Elliott Company in Jeannette, Pennsylvania, where he specializes in rotorbearing system dynamics. He has been with Elliott Company since 1995. Mr. Pettinato's responsibilities include lateral and torsional rotordynamic analyses, and the testing and evaluation of bearing, squeeze-film damper, and seal designs. Prior to joining Elliott Company, he worked as a project engineer for an aftermarket bearing manufacturer.

Mr. Pettinato received his BSME (1989) and MSME (1992) degrees from the University of Virginia. He has written several technical papers and is a registered Professional Engineer in the State of Pennsylvania. He is a member of ASME and STLE, and is the current Vice-Chairman of the Pittsburgh Section of STLE.

Pranabesh De Choudhury has worked for Elliott Company in Jeannette, Pennsylvania, for the past 31 years in the area of rotorbearing system dynamics. In his current position as Senior Consulting Engineer, his responsibilities include rotorbearing dynamics, bearing design and analysis, torsional dynamics, blade vibration analysis, and troubleshooting field vibration problems.

Dr. De Choudhury obtained a BSME (1963) from Jadavpur University, Calcutta, India, an MSME from Bucknell University, and his Ph.D. (Mechanical Engineering, 1971) from the University of Virginia. He has written several technical papers, and has been awarded a patent. He is a registered Professional Engineer in the State of Pennsylvania, and is a member of ASME and STLE.

ABSTRACT

A series of performance, unbalance response, and stability tests were performed on a flexible rotor incorporating two flexure pivot tilt-pad journal bearings, followed by a theoretical correlation using synchronous and frequency dependent bearing characteristics. The test data consisting of Bodé plots and frequency cascade plots are presented along with measured bearing performance data, including peak temperatures at different speeds.

Unbalance tests consisted of applying a midspan unbalance. Effects of oil inlet flowrate and oil inlet temperature are examined. The measured peak responses are compared to the theoretical in five measurement planes.

Stability tests consisted of running the balanced rotor up in speed to provide a high flexibility ratio and reduced logarithmic decrement. For these cases, the motion of the rotor was measured in five planes and results are presented in the form of cascade diagrams. The tests were conducted under a series of operation conditions by varying the speed, oil inlet temperature, and flowrates. High amplitude resonant whip instability did not occur; however, low amplitude limit cycle instability did occur, which aided in determining the stability threshold. Correlation of the test results to the theoretical logarithmic decrement was performed using both synchronous and nonsynchronous bearing coefficients, both with and without pivot rotational stiffness. Based on the results of this study, the theoretical model with the nonsynchronous bearing coefficients best represents the rotorbearing system. Pivot rotational stiffness had little effect.

INTRODUCTION

Dynamic characteristics of high-speed turbomachinery are largely dependent upon bearing dynamic characteristics both in terms of unbalance response and stability. This has resulted in numerous studies conducted on bearing dynamic characteristics for improved analysis and improved bearing design. One area that has not been adequately addressed, however, is the effect of frequency dependence in tilt-pad journal bearings.

With regard to flexure pivot journal bearing applications, logarithmic decrements cited in literature have been fairly high and were cited to be in excess of 0.3 for two integrally geared applications (De Choudhury, et al., 1992; Chen, et al., 1994), and in excess of 1.4 for a turboexpander application (Kardine, et al., 1996). The analytical results that have been presented are limited to synchronously reduced coefficients and do not include the effect of frequency dependence on the tilt-pad journal bearing coefficients. In order to further determine the stability characteristics of these bearings and thus define the bearing application envelope, a series of tests was conducted.

This paper details performance, unbalance response, and stability characteristics of a pair of flexure pivot journal bearings supporting a flexible shaft. The effect of speed (0 to 15,000 rpm), oil inlet temperature (110°F, 120°F, 130°F), and oil inlet flowrate (1.5 gpm, 2 gpm, 2.5 gpm) are examined. Steady-state performance is reported in the form of power loss and bearing metal temperatures. Unbalance response data are presented in the form of Bodé diagrams. Stability results are shown as cascade plots.

A detailed theoretical analysis is performed, and results are compared to the test data. The flexure pivot tilt-pad journal bearings are modeled using both synchronous and nonsynchronous coefficients. While fixed geometry journal bearings have no

observable frequency dependent characteristics (Pettinato, et al., 2001), tilt-pad journal bearing coefficients are theoretically frequency dependent (Smalley, et al., 1975; Raimondi and Szeri, 1984; Barrett, et al., 1988), such that the bearing coefficients can be significantly different at the instability whirl frequency as compared to the operational speed of the machine. Consequently, from a standpoint of stability analysis, this can lead to significantly different results depending on whether synchronous or nonsynchronous reduction frequencies are used. Unfortunately, there has been little evidence either for or against the frequency dependent mathematical model (Nicholas, 2001). This has resulted in an ongoing debate as to whether synchronous or nonsynchronous coefficients should be used for stability analysis. But while the frequency dependence of tilt-pad journal bearing coefficients remains a controversial topic, the authors believe that this is primarily due to a lack of benchmarking using both methods. It should be noted that techniques involving the use of synchronous coefficients (Rouch, 1983; Wachel, 1986; Nicholas, 2001) and nonsynchronous coefficients (De Choudhury, 2001; Rouch, 1983) have been used for stabilizing flexible machinery. Depending on the bearings used, the use of one method over another could lead to either an overly conservative or overly aggressive limitation on logarithmic decrement. Given current state-of-the-art, it is beneficial to examine both methods. As such, the theoretical analysis consists of four bearing models—with and without pivot rotational stiffness, as well as with and without frequency dependence for purposes of benchmarking the series of tests performed.

Test Stand Design and Configuration

A highly flexible rotor was used to perform the stability tests. The test rig (Figure 1) consisted of a variable speed motor driving a shaft through a flexible coupling. The shaft was supported by two journal bearings 34 inches apart. The coupling end bearing is termed the DE (drive-end) bearing, while the free end bearing is termed the NDE (nondrive-end) bearing. The shaft consisted of 2.93 inch diameter journals, and a 2.375 inch diameter center section. One 9 inch diameter and two 12 inch diameter disks were mounted between bearings near the shaft center, thus providing a highly flexible shaft with first stiff support critical at 3937 rpm. An empirical parameter used as a stability criterion is the flexibility ratio defined as the ratio of shaft operating speed, N, to the first critical speed on stiff supports, Nc1 (Sood, 1979). The flexibility ratio of the test rotor, N/Nc1, is 3.81 at 15,000 rpm, which is well outside the typical experience range for operation without external damping.

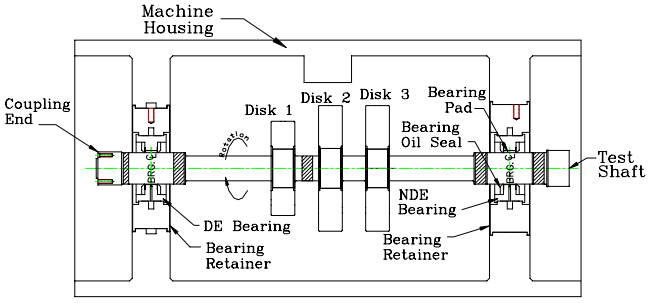

Figure 1. Flexible Rotor Test Stand.

The rotor itself was incrementally balanced by first balancing the shaft alone, and then balancing the assembly as each successive disk was added. Table 1 describes the rotordynamic characteristics of the flexible shaft design.

The test stand was instrumented with 10 eddy-current probes sensing in five planes. The sensor plane locations are shown in Figure 1 as hatched regions. Two probes were located at the shaft center ±45 degrees from bottom dead center. A pair of probes was also located inboard and outboard of each bearing, sensing in vertical and horizontal directions. Each bearing was instrumented with thermocouples embedded in the two loaded pads. Bearing inlet flowrates were monitored using positive displacement flowmeters. The inlet flowrate was adjusted by varying oil inlet pressure.

Table 1. Shaft Design with Three Disks.

1st Stiff Support Critical Speed, Nc1 (cpm)	3937
2nd Stiff Support Critical Speed, Nc2 (cpm)	17115
Flex Ratio, N/Nc1, at 15,000 RPM (dim)	3.81
Drive End (DE) Bearing Load (lb)	137.9
Non Drive End (NDE) Bearing Load (lb)	124.5

Bearing Design

The rotor was supported on two flexure pivot tilt-pad journal bearings. Both the drive-end and nondrive-end bearings were of the same design. One such bearing is shown in Figures 2 and 3. The bearings were four-pad, center pivot design, and were machined by wire electrical discharge machining (EDM) such that the pads were integral to the bearing shell. The bearings were lightly loaded with 137.9 lb loading (41 psi) on the drive-end bearing, and 124.5 lb loading (37 psi) on the nondrive-end bearing. Details of the bearing design are provided in Table 2. The bearings were designed with low preload (0.111).

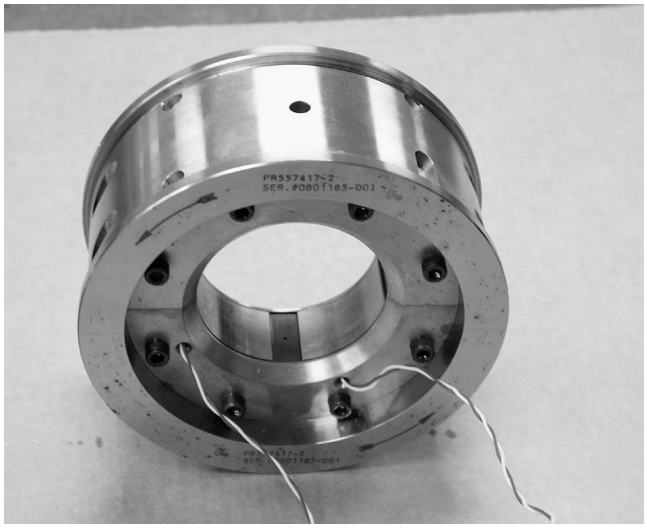

Figure 2. Bearing Assembly.

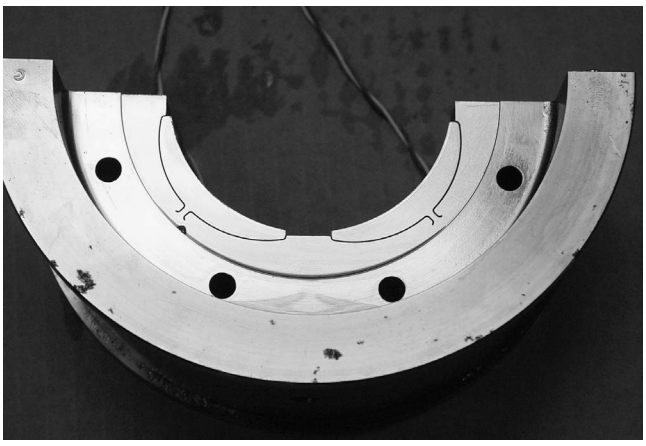

Figure 3. Disassembled Bearing Half.

Table 2. Flexure Pivot Tilt-Pad Journal Bearing Design.

Bearing Type	4 Shoe Tilt-pad		
Journal Diameter, D	2.9533 +0/-.0005 inch		
Pad Length, L	1.140 inch		
L/D	0.386		
Pad Arc, α	72°		
Offset Factor, χ	0.5		
Pivot Type	Flexure		
Pivot Radial Stiffness	16,300,000 lb/in		
Pivot Rotational Stiffness	4,896 inch-lb/rad		
Diametral Seal Clearance, C_s	0.0127 – 0.0153		
	Min. Clr., Max. Prld.	Nom. Clr., Nom. Prld.	Max Clr., Min. Prld.
Diametral Bearing Clearance, C_b	0.0035	0.0040	0.0045
Diametral Pad Clearance, C_p	0.0045	0.0045	0.0045
Preload, m	0.222	0.111	0.000

Lubricant Properties

The lubricant used was ISO VG-32 light turbine oil. Viscosity measurements were made in accordance with ASTM D445. The lubricant viscosity measured 34.681 cst at 100°F, 11.859 cst at 155°F, and 5.653 cst at 210°F. The specific gravity was 0.8602 at 60°F.

Experimental Procedure

The rotor was runup in the balanced state from 0 rpm to 15,000 rpm in increments of 1000 rpm for steady-state data collection consisting of oil inlet pressure, temperature, flowrate, bearing thermal power loss, and pad metal temperatures. After steady-state data collection, the rotor was again runup from 0 rpm to 15,000 rpm under constant acceleration for collection of vibration data consisting of amplitude, phase, and spectral data. The balanced rotor was used to assess the stability of the rotorbearing system, since presence of unbalance can be stabilizing as noted by Barrett, et al. (1976).

Unbalance response sensitivity was also examined by applying unbalance amounts, which were approximately eight times the 0.07 oz-in residual unbalance. The first unbalance set consisted of the static unbalance case with 0.546 oz-in applied at the center disk. The second unbalance set consisted of the dynamic unbalance case with 0.274 oz-in applied at disk one and 0.281 oz-in applied 180 degrees out-of-phase at disk three. The third unbalance set consisted of approximately eight times overhung unbalance or 0.048 oz-in applied at the coupling adapter.

The procedures for stability and unbalance response were repeated under a series of conditions including flowrates of 1.5, 2.0, and 2.5 gpm; and inlet oil temperatures of 110°F, 120°F, and 130°F. The selected flowrates bracketed the range of flows typically specified for machines operating under these conditions. The inlet oil temperatures used include the nominal temperature case of 120°F, plus additional cases to determine sensitivity to oil inlet viscosity.

RESULTS

Both the analytical and experimental data are presented for the purpose of correlation study. The results consist of steady-state bearing performance data, unbalance response as measured at each plane for each set of unbalance, and stability.

Analytical Model

The rotor was modeled assuming a massless shaft with finite stiffness. Assembled parts (impellers, rotor blade or disk, sleeves, couplings, etc.) and shaft mass were represented by concentrated masses as discussed by De Choudhury, et al. (1976). The rotor model and critical speed map are shown in Figures 4 and 5, respectively. Bearings were modeled as simple "spring-damping pot" systems from data generated by thermohydrodynamic (THD) analysis (Branagan, 1988) with adiabatic boundary condition between the film and pad. Effects of unloaded pads were ignored.

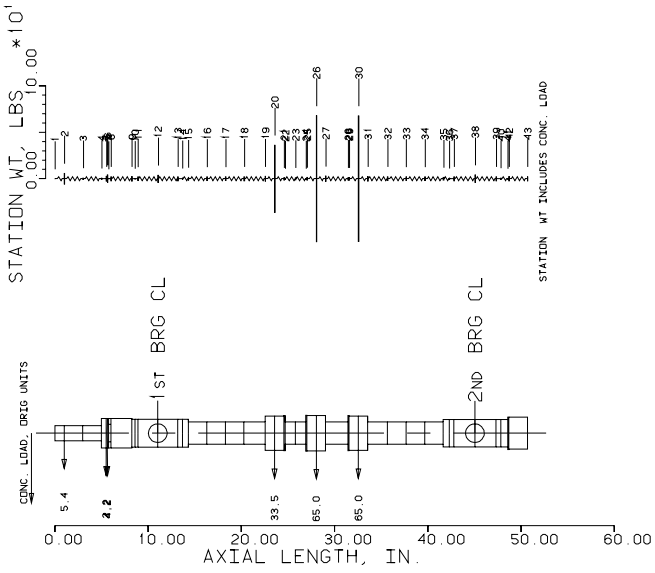

Figure 4. Rotor Model.

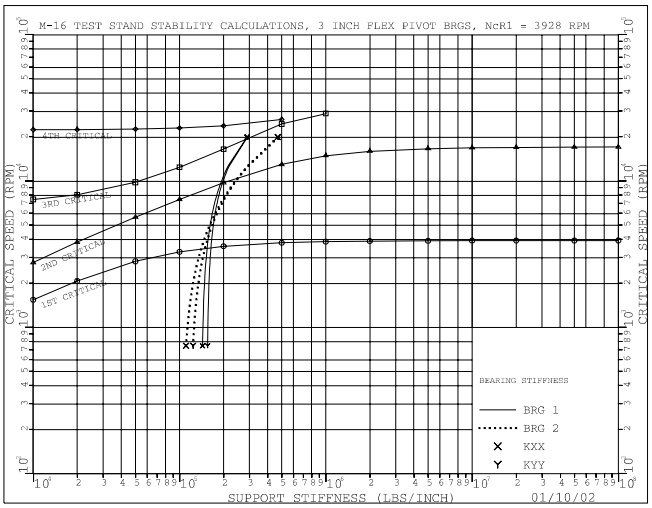

Figure 5. Critical Speed Map.

As noted, the bearing coefficients were determined using both synchronous and nonsynchronous reduction frequencies, with and without pivot rotational stiffness. The nonsynchronous reduction frequency was selected as 4000 cpm, to coincide with the first critical speed. Results of the bearing analysis are shown in Figures 6 through 13 in the "Lund" coordinate system with *x* in the load direction and *y* in the horizontal direction. Observable discontinuities in the plots coincided with loading of upper pads. Examination of the figures shows that use of the nonsynchronous (4000 cpm) reduction frequency resulted in theoretically higher principal stiffness and lower principal damping as compared to the synchronous coefficients. Synchronous and nonsysnchronous coefficients coincided at 4000 rpm shaft speed since the reduction frequencies are identical at this speed. The 4896 in-lb/rad pivot rotational stiffness resulted in significant amounts of cross-coupling, which can be destabilizing as expected.

Steady-State Performance

Some steady-state results are presented in Figures 14 and 15, and summarized in Table 3. The experimentally derived power loss was in fairly good agreement with the theoretical. Bearing thermal power loss generally decreased with increasing oil inlet temperature (decreasing inlet oil viscosity) as would be expected.

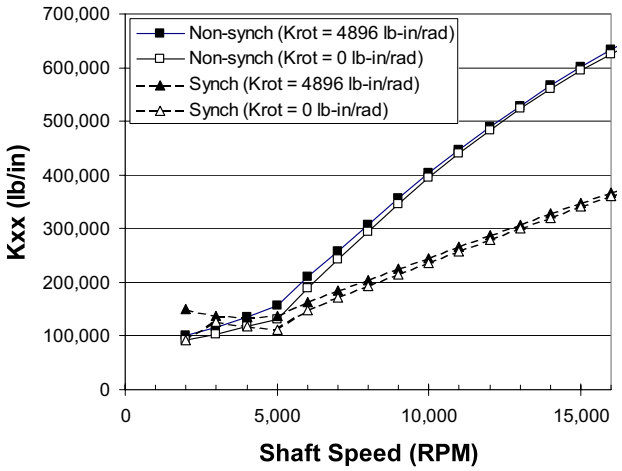

Figure 6. Kxx Versus Shaft Speed.

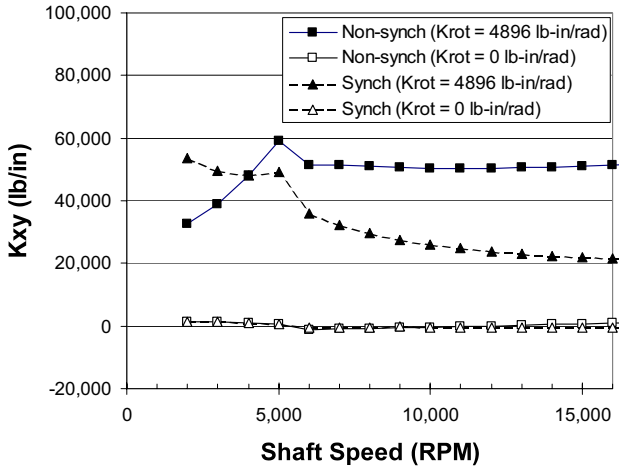

Figure 7. Kxy Versus Shaft Speed.

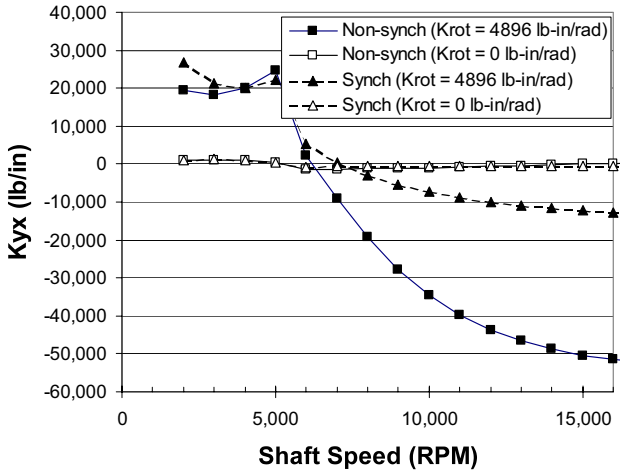

Figure 8. Kyx Versus Shaft Speed.

Bearing metal temperature increased with speed. Higher inlet temperature generally resulted in higher pad metal temperature; however, the effect of inlet oil temperature on pad metal temperature diminished with increasing speed such that at maximum operating speed, the inlet temperature had essentially no effect on pad metal temperature. Predicted bearing temperature was considerably less than the measured per the program used; however, measured data were within empirical predictions typically used by the turbomachinery OEM.

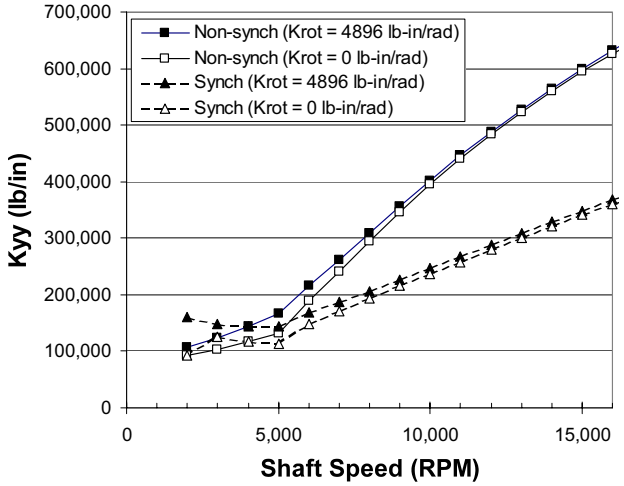

Figure 9. Kyy Versus Shaft Speed.

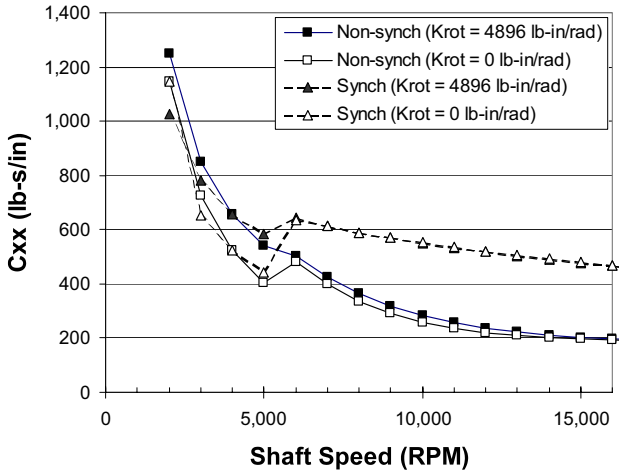

Figure 10. Cxx Versus Shaft Speed.

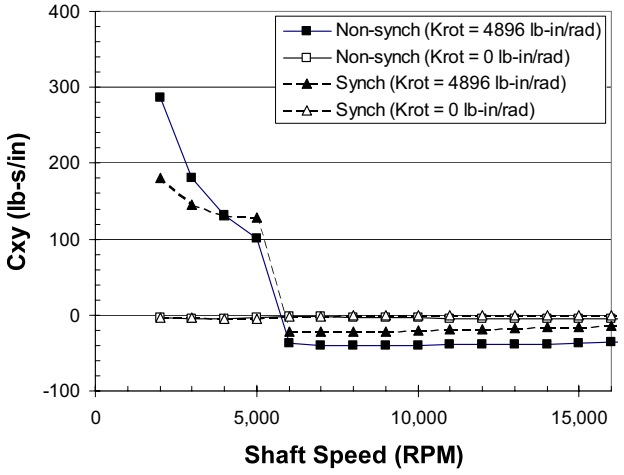

Figure 11. Cxy Versus Shaft Speed.

Unbalance Response

The experimental unbalance response results are presented as Bodé plots in Figures 16 and 17 for an oil inlet flowrate of 2.5 gpm with center unbalance. Each curve consists of resultant data after the point-by-point subtraction of the residual unbalance Bodé plot as detailed by Nicholas, et al. (1997). Figure 16 shows the five different measurement planes, horizontal direction for the nominal temperature of 120°F and oil inlet flowrate of 2.5 gpm when using

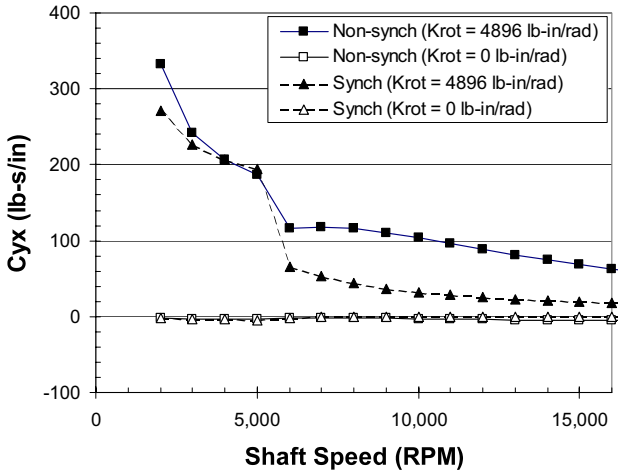

Figure 12. Cyx Versus Shaft Speed.

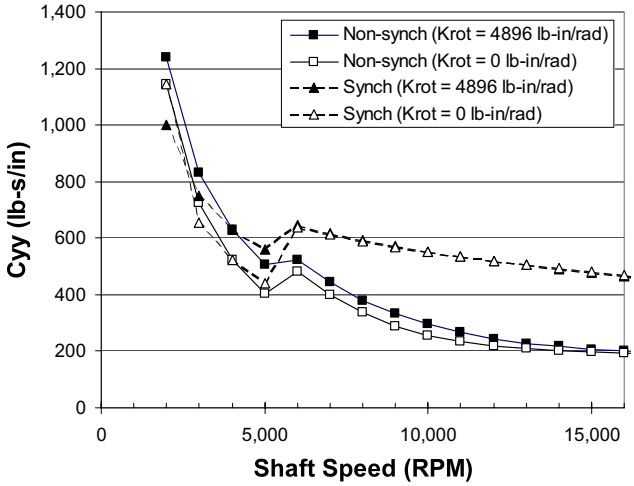

Figure 13. Cyy Versus Shaft Speed.

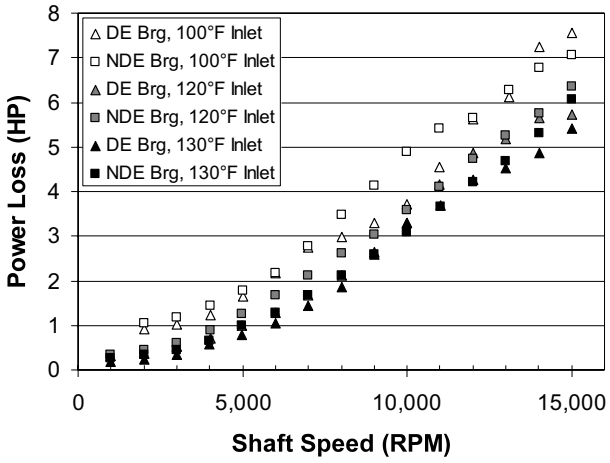

Figure 14. Power Loss Versus Speed and Oil Inlet Temperature.

midspan unbalance. Unbalance response increases when moving from the outboard planes toward the center of the rotor. Figure 17 shows the theoretical data, accounting for pivot rotational stiffness, as well as measured data observed at the center probe location. Results are presented in greater detail in Table 4 for the 120°F case detailing speeds and amplitudes of the first critical speed as observed at each of the 10 probes with midspan unbalance.

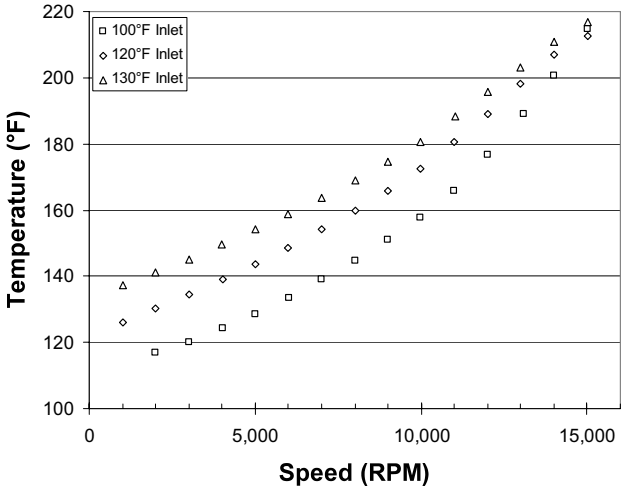

Figure 15. Pad Temperature Versus Speed and Oil Inlet Temperature (NDE Bearing, Trailing Pad, 75 Percent Location, 2.5 GPM).

Table 3. Steady-State Results, 120°F Oil Inlet Temperature at 2.5 GPM, 15000 RPM, Balanced Rotor.

	Power Loss (HP)			Max Bearing Metal Temp. (°F)		
				Test Data		
	Test	Theory	% Diff.	Leading Pad	Trailing Pad	Theory
DE Bearing	5.14	5.69	10.7	197.1	191.5	179
NDE Bearing	6.5	5.67	-12.8	211.8	218.2	165

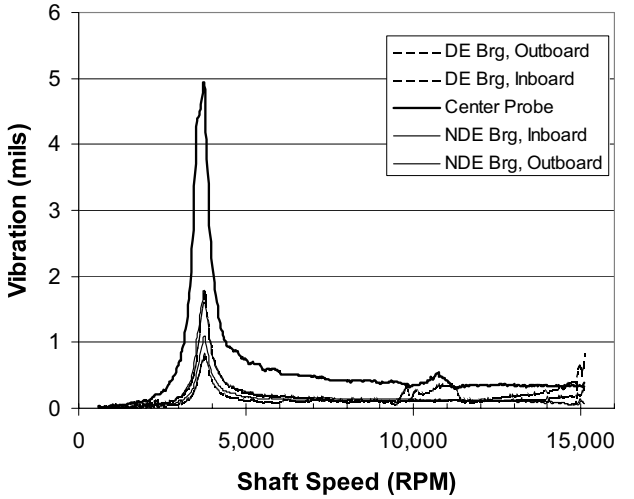

Figure 16. Bodé Plot, Horizontal Probes, Midspan Unbalance, 2.5 GPM, 120°F Oil Inlet Temperature.

API Standards require unbalance response prediction of critical speeds to within ±5 percent of the measured. These limitations could be regarded as stringent by some researchers. Vance (1987) notes that prediction of the first three critical speeds to within 7 percent should be practical. Nicholas, et al. (1997), performed correlation of predicted and measured unbalance response on five different industrial machines. While results were typically within the 5 percent range, discrepancies of up to 10.8 percent were noted.

For the test results presented herein, critical speeds were predicted within ±5.7 percent on average. Predicted critical speeds for the horizontal direction were all within 4 percent of the measured. Amplitudes were underpredicted by 3.9 percent on average.

Additional unbalance response cases for the dynamic unbalance and coupling unbalance are detailed in Figures 18 and 19.

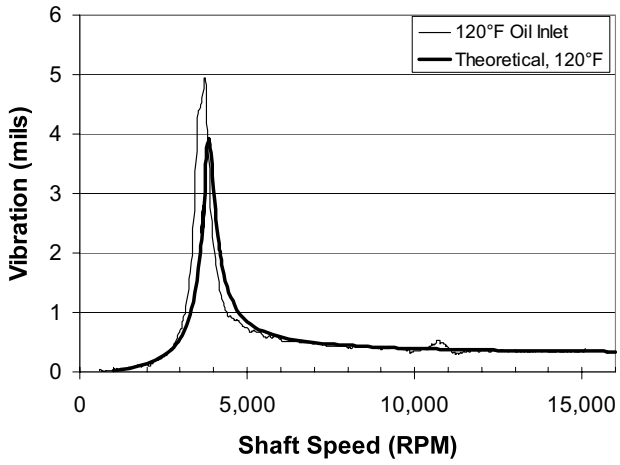

Figure 17. Bodé Plot, Horizontal Center Probe, Midspan Unbalance, 2.5 GPM, 120°F Oil Inlet Temperature.

Table 4. Theoretical and Experimental Unbalance Response Data, Midspan Unbalance, 2.5 GPM, 120°F Oil Inlet Temperature.

		Theoretical		Experimental With Runout Subtraction Of The Residual Unbalance Case	
Probe Location	Probe Angle	1st Critical Speed (rpm)	1st Critical Amp (mils p-p)	1st Critical Speed (rpm)	1st Critical Amp (mils p-p)
DE Brg. Outboard	Vert	3825	0.66	3520	0.50
	Horiz	3900	0.75	3750	0.58
DE Brg. Inboard	Vert	3825	1.17	3500	1.16
	Horiz	3900	0.91	3750	1.25
Center Probe	225°	3825	3.92	3770	3.85
	315°	3900	2.49	3750	4.94
NDE Brg. Inboard	Vert	3825	1.26	3520	1.22
	Horiz	3900	0.99	3750	1.27
NDE Brg. Outboard	Vert	3825	0.78	3520	0.67
	Horiz	3900	0.84	3750	1.10

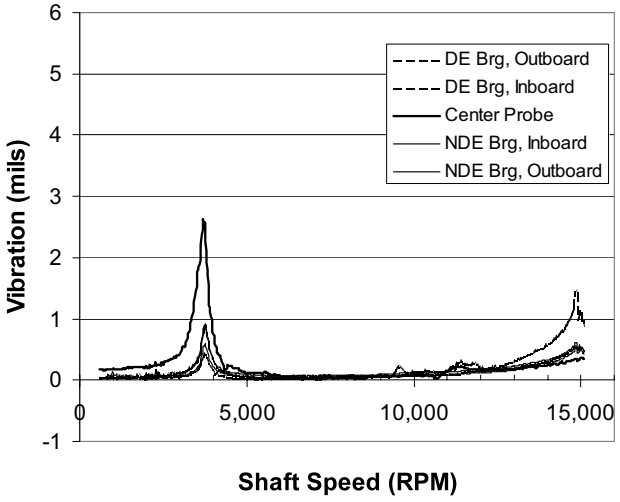

Figure 18. Bodé Plot, Horizontal Probes, Dynamic Unbalance, 2.5 GPM, 120°F Oil Inlet Temperature.

Stability Results

The experimental stability results are presented as cascade plots in Figures 20 through 22 for an oil inlet flowrate of 2.5 gpm and an oil inlet temperature of 120°F. Results are summarized in Table 5 for each probe, showing the maximum subsynchronous vibration amplitude recorded, including the frequency of the vibration and the speed at which it was noted, as well as the synchronous

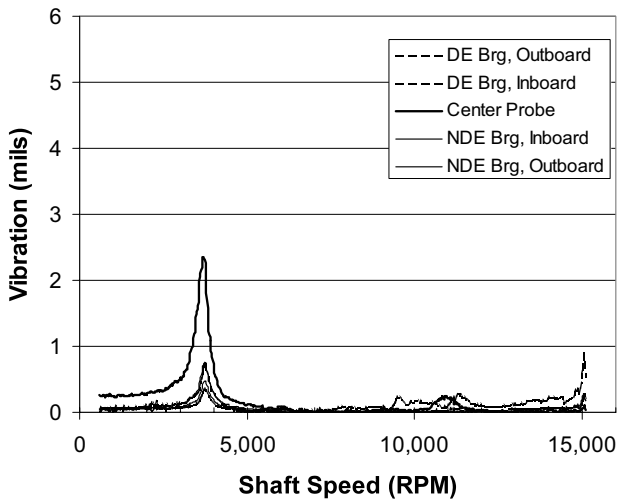

Figure 19. Bodé Plot, Horizontal Probes, Coupling Unbalance, 2.5 GPM, 120°F Oil Inlet Temperature.

vibration at the same speed. The synchronous vibration amplitudes presented in Table 5 are adjusted for vector runout subtraction.

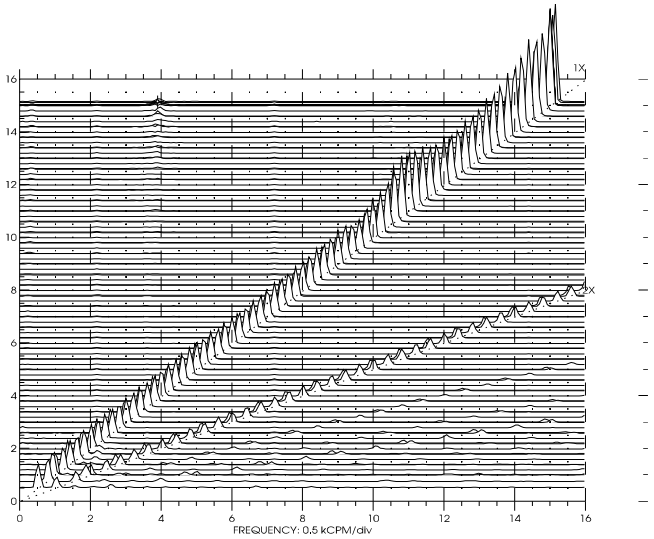

Figure 20. Cascade Plot, Main Bearing, Outboard, 2.5 GPM, 120°F Oil Inlet Temperature.

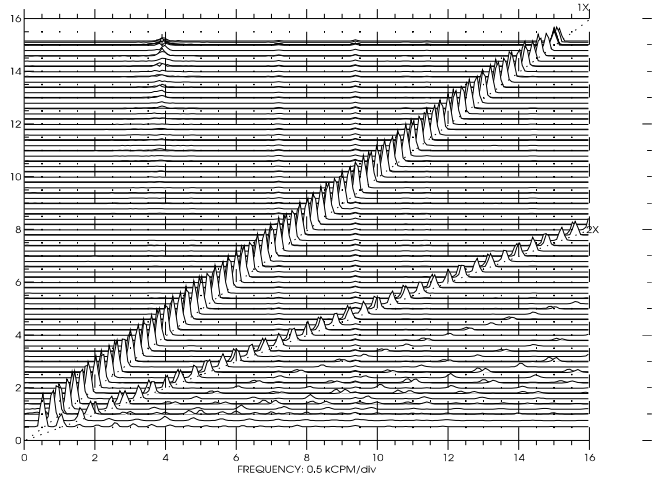

Figure 21. Cascade Plot, Test Bearing, Outboard, 2.5 GPM, 120°F Oil Inlet Temperature.

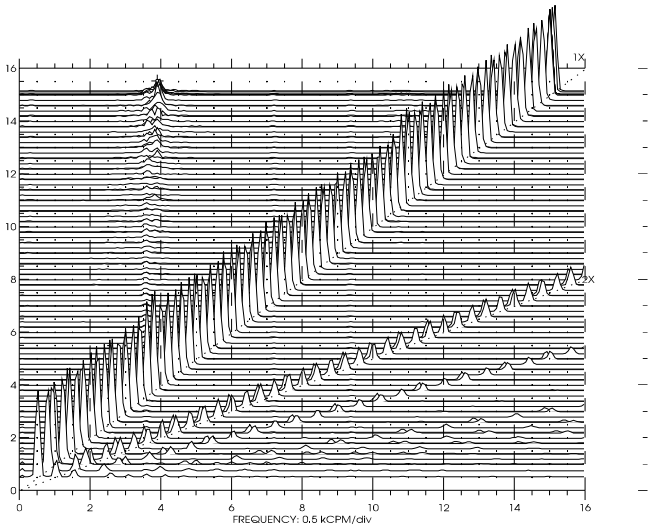

Figure 22. Cascade Plot, Center Probe, 2.5 GPM, 120°F Oil Inlet Temperature.

Table 5. Vibration Characteristics at Speed with Maximum Subsynchronous Vibration (120°F Oil Inlet Temperature and 2.5 GPM Flowrate).

Probe Location	Probe Orientation	Rotor Speed (rpm)	Synchronous Vibration Amplitude (mils, pk-pk)	Subsynchronous Vibration Amplitude (mils, pk-pk)	Subsynchronous Vibration Frequency (cpm)
DE Brg. Outboard	Vertical	14600	1.04	0.04	3900
	Horizontal	14600	1.16	0.10	3900
DE Brg. Inboard	Vertical	14600	0.36	0.06	3900
	Horizontal	14600	0.31	0.17	3900
Center Probe	–45°	14600	0.35	0.54	3825
	+45°	14600	0.28	0.45	3825
NDE Brg. Inboard	Vertical	14600	0.44	0.07	3900
	Horizontal	14600	0.39	0.16	3900
NDE Brg. Outboard	Vertical	14600	0.31	0.06	3900
	Horizontal	14600	0.37	0.14	3900

Examination of the data shows that the occurrence of high amplitude instability, known as resonant whip, did not occur for any of the cases. However, there was presence of low amplitude limit cycle instability (Figures 20 to 22), as indicated by the presence of subsynchronous vibration that was lower in amplitude than the synchronous. The direction of precession was noted as forward. As shown in Figure 22, the subsynchronous whirl frequency tended to increase very slightly with speed. The corresponding subsynchronous vibration amplitude generally increased with speed as well, and was most prevalent at maximum speed. The system was therefore only marginally stable.

Tables 6 and 7 detail the effect of oil inlet temperature and oil inlet flowrate on the subsynchronous vibration amplitudes and threshold speeds. An arbitrary threshold level of 0.10 mils was used to quantify the results shown in Tables 6 and 7. In this case, the threshold speed was defined to be the speed at which the subsynchronous vibration exceeded 0.10 mils at the center probe. While 0.10 mils could be considered a small amplitude, the tables indicate that it is a significant percentage of the synchronous vibration. This is not clear from the figures because runout is not subtracted in the cascade diagrams.

Table 6. Effect of Oil Flowrate on Stability.

Oil Inlet			Threshold Speed (rpm)	Data At Corresponding Threshold Speed				Max. Subsynch Amp. Over Speed Range (mils, p-p)
Flow Rate (gpm)	Press (psig)	Temp (°F)		Flex Ratio	Synch. Vib. Amp. (mils, p-p)	Subsynch. Vib. Amp. (mils, p-p)	Subsynch. Vib. Freq. (cpm)	
2.5	25.4	120	11000	2.79	0.185	0.113	3825	0.535
2.0	17.9	120	11900	3.02	0.206	0.154	3975	0.432
1.5	10.7	120	12100	3.07	0.113	0.113	3900	0.350

Table 7. Effect of Oil Inlet Temperature on Stability.

Oil Inlet			Threshold Speed (rpm)	Data At Corresponding Threshold Speed				Max. Subsynch Amp. Over Speed Range (mils, p-p)
Flow Rate (gpm)	Press (psig)	Temp (°F)		Flex Ratio	Synch Vib. Amp. (mils, p-p)	Subsynch Vib. Amp. (mils, p-p)	Subsynch Vib. Freq. (cpm)	
2.5	24.6	130	12800	3.25	0.216	0.134	3600	0.452
2.5	25.4	120	11000	2.79	0.185	0.113	3825	0.535
2.5	26.6	110	11400	2.90	0.164	0.113	3900	0.421

As detailed in Tables 6 and 7, differences were noted between the various inlet oil temperatures and flowrates. In particular, the amplitudes and the onset speed of the low amplitude limit cycle instability were affected by oil inlet temperature and oil inlet flowrate. Based on the acquired data, the maximum subsynchronous vibration amplitude was 0.54 mils peak-to-peak at a flowrate of 2.5 gpm and an oil inlet temperature of 120°F. The minimum threshold speed was 11,000 rpm, which corresponded to a flexibility ratio of 2.79. As shown in Table 6, decreasing flowrate was accompanied by an increase in the threshold speed and a decrease in the maximum subsynchronous vibration amplitude observed over the speed range. This could also be due to decreased bearing housing oil pressure. As shown in Table 7, there is no clear effect of temperature on either the threshold speed or maximum amplitudes of subsynchronous vibration.

Theoretical Stability Results

The stability of the rotorbearing system was evaluated over the speed range, and is presented as the logarithmic decrement (log dec), Δ, which is a measure of the damping in the rotorbearing system. A positive logarithmic decrement indicates a stable rotorbearing system while a negative logarithmic decrement indicates an unstable system. Typically, instability will result in whirling of the rotor at the first natural frequency.

The results are presented with respect to speed using both synchronous and nonsynchronous bearing coefficients (Figure 23). Results of the two methods are similar where bearing coefficients are similar, namely at speeds less than 6000 rpm. At speeds greater than 6000 rpm, the predicted stability results using the two methods become progressively divergent in conjunction with similar divergence in bearing coefficients. At the maximum operating speed of 15,000 rpm, the synchronous method predicts significantly higher logarithmic decrement as compared to the nonsynchronous method, as expected. And whereas the synchronous data generally predict a stable rotor system, the nonsynchronous data show that the system is marginally stable, which is most in agreement with the experimental data. The theoretical reduction in stability is to be expected since the bearing principal damping coefficients (Figures 10 and 13) show a significant decrease when considering frequency dependence. Also, the bearing principal stiffness coefficients (Figures 6 and 9) show a significant increase when considering frequency effects. The net result is to reduce damping at the bearings as well as the effectiveness of that damping, thus causing decreased system stability. The addition of the theoretical 4896 lb-in/rad pivot rotational stiffness into the theoretical model had little effect on theoretical stability.

Evaluating the case with synchronous coefficients shows that the predicted logarithmic decrement was 0.252 at the onset of limit cycle instability (11,000 rpm). Whereas the case with nonsynchronous coefficients shows that the predicted logarithmic decrement was 0.038 at the onset of limit cycle instability (11,000 rpm). As such, the nonsynchronous analysis is most valid for the rotorbearing system tested. Results for the instability threshold speed are shown in Table 8. As noted, the inclusion of pivot rotational stiffness had only minor effect on the logarithmic decrement. It is of interest that inclusion of pivot rotational stiffness had a theoretically destabilizing effect when applied to the nonsynchronous coefficients, but a theoretically stabilizing effect when applied to the synchronous coefficients.

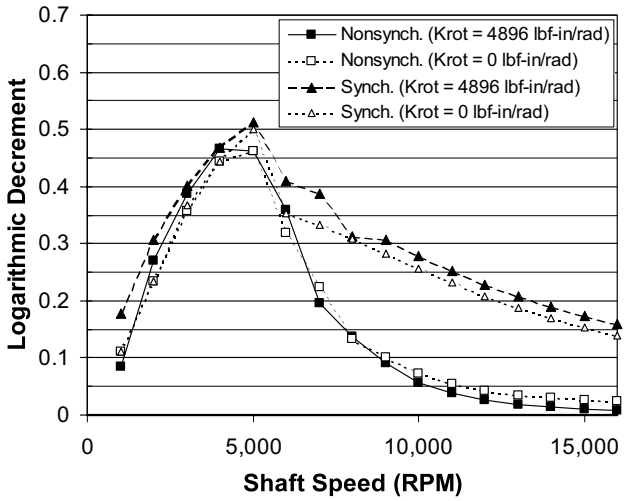

Figure 23. Logarithmic Decrement Versus Speed.

Table 8. Logarithmic Decrement Results at 11,000 RPM Instability Threshold Speed.

Case	Log Dec
Nonsynchronous with Pivot Rotational Stiffness	0.038
Nonsynchronous without Pivot Rotational Stiffness	0.054
Synchronous with Pivot Rotational Stiffness	0.252
Synchronous without Pivot Rotational Stiffness	0.231

The whirl frequency versus speed is presented in Figure 24 for both the synchronous and nonsynchronous evaluations, and for the experimental data. As shown, the theoretical whirl frequency is fairly constant when considering the synchronous coefficients, but increases more pronouncedly when considering the nonsynchronous coefficients, approaching the theoretically rigid support case (Nc1 = 3937 rpm). The experimental data are included in the plot, but have considerable scatter. Still, the overall trend as depicted by the experimental data best matches the case using the nonsynchronous coefficients. The pivot rotational stiffness included in the theoretical model had little effect on the whirl frequency.

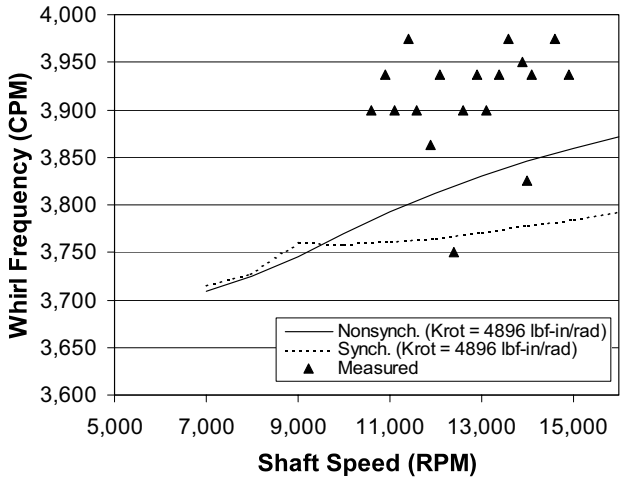

Figure 24. Whirl Frequency Versus Speed.

CONCLUSIONS

A pair of 2.95 × 1.14 inch flexure pivot tilt-pad journal bearings was tested on a flexible rotor test stand over a range of speeds, oil inlet temperatures, and oil inlet flowrates. These tests showed the following:

Steady-State

- Bearing thermal power loss generally decreased with increasing oil inlet temperature.
- Program predicted bearing temperatures at 15,000 rpm (179°F, 165°F) were considerably less than the measured temperatures at either the DE bearing (197°F) or NDE bearing (218°F).
- Program prediction of temperature was not as accurate as empirical methods.
- Higher inlet temperature generally resulted in higher metal temperature; however, at the maximum continuous speed, the inlet temperature had essentially no effect on pad metal temperature.

Unbalance Response

- The average percent difference between measure and predicted critical speeds was 5.7 percent.
- The average percent difference between measure and predicted amplitudes was 3.9 percent.

Stability

- The system exhibited low amplitude, limit cycle instability.
- The stability of the system was somewhat sensitive to oil inlet flowrate from 1.5 gpm to 2.5 gpm while holding the inlet temperature constant at 120°F. The minimum stability threshold speed for limit cycle instability was noted at 11,000 rpm at 2.5 gpm, which corresponds to a flex ratio of 2.79. Higher oil inlet flowrates resulted in reduced stability threshold.
- The stability of the system was sensitive to oil inlet temperature from 110°F to 130°F while holding the inlet flowrate constant at 2.5 gpm.
- Modeling of the pivot rotational stiffness had only a slight effect on the predicted rotorbearing system stability, and may only need to be included when designing near the edge of stability criterion.
- Inclusion of frequency dependence in the bearing model via nonsynchronous reduction frequency had a significant effect on the predicted rotorbearing system stability.
- The low amplitude, limit cycle instability was most in agreement with the prediction using theoretical nonsynchronous bearing coefficients and including pivot rotational stiffness.
- The general increase in whirl frequency exhibited by the rotorbearing system was most in agreement with the model employing nonsynchronously reduced bearing coefficients.
- Stability prediction based on synchronously reduced bearing coefficients provides theoretically higher and more optimistic logarithmic decrement values as compared to the nonsynchronously reduced bearing coefficients.

Overall, there was good agreement between the prediction and the experimental onset of instability when using the nonsynchronously reduced bearing coefficients.

REFERENCES

Barrett, L. E., Akers, A., and Gunter, E. J., 1976, "Effect of Unbalance on a Journal Bearing Undergoing Oil Whirl," Proceedings of the IMechE, *190*, pp. 535-543.

Barrett, L. E., Wilson, B. W., and Allaire, P. E., 1988, "The Eigenvalue Dependence of Reduced Tilting Pad Bearing Stiffness and Damping Coefficients," Tribology Transactions, *31*, pp. 411-419.

Branagan, L. A., 1988, "Thermal Analysis of Fixed and Tilting Pad Journal Bearings Including Cross-Film Viscosity Variations and Deformation," Ph.D. Dissertation, University of Virginia, Charlottesville, Virginia.

Chen, W. J., Zeidan, F. Y., and Jain, D., 1994, "Design, Analysis, and Testing of High Performance Bearings in a High Speed Integrally Geared Compressor," *Proceedings of the Twenty-Third Turbomachinery Symposium*, Turbomachinery Laboratory, Texas A&M University, College Station, Texas, pp. 31-42.

De Choudhury, P., 2001, "Application of Lund's Stability Analysis Program in Design of Modern Turbomachinery," DETC2001/VIB21374.

De Choudhury, P., Hill, M. R., and Paquette, D. J., 1992, "A Flexible Pad Bearing System for a High Speed Centrifugal Compressor," *Proceedings of the Twenty-First Turbomachinery Symposium*, Turbomachinery Laboratory, Texas A&M University, College Station, Texas, pp. 57-64.

De Choudhury, P., Zsolcsak, S. J., and Barth, E. W., 1976, "Effect of Damping on the Lateral Critical Speeds of Rotor Bearing Systems," ASME Journal of Engineering for Industry, pp. 505-513.

Kardine, W. A., Agahi, R. R., Ershagi, B., and Zeidan, F. Y., 1996, "Application of High Speed and High Efficiency Hydrogen Turboexpanders in Refinery Service," *Proceedings of the Twenty-Fifth Turbomachinery Symposium*, Turbomachinery Laboratory, Texas A&M University, College Station, Texas, pp. 95-101.

Nicholas, J. C., 2001, "Lund's Pad Assembly Method for Tilting Pad Journal Bearings," DETC2001/VIB-21371.

Nicholas, J. C., Edney, S. L., Kocur, J. A., and Hustak, J. F., 1997, "Subtracting Residual Unbalance for Improved Test Stand Vibration Correlation," *Proceedings of the Twenty-Sixth Turbomachinery Symposium*, Turbomachinery Laboratory, Texas A&M University, College Station, Texas, pp. 7-18.

Pettinato, B. C., Flack, R. D., and Barrett, L. E., 2001, "Effect of Excitation Frequency and Orbit Magnitude on the Dynamic Characteristics of a Highly Preloaded Three-Lobe Journal Bearing," Tribology Transactions, *44*, pp. 575-582.

Raimondi, A. A., and Szeri, A. Z., 1984, "Journal and Thrust Bearings," *Handbook of Lubrication (Theory and Practice of Tribology) Volume II Theory and Design*, CRC Press, Inc., pp 413-462.

Rouch, K. E., 1983, "Dynamics of Pivoted-Pad Journal Bearings, Including Pad Translation and Rotation Effects," ASLE Transactions, *26*, pp. 102-109.

Smalley, A. J., Almstead, L. G., Lund, J. W., and Koch, E. S., 1975, "User's Manual MTI Cadense Program CAD-25, Dynamic Stability of a Flexible Rotor," Mechanical Technologies Incorporated, Latham, New York.

Sood, V. K., 1979, "Design and Full Load Testing of a High Pressure Centrifugal Natural Gas Injection Compressor," *Proceedings of the Eighth Turbomachinery Symposium*, Turbomachinery Laboratory, Texas A&M University, College Station, Texas, pp. 35-42.

Vance, J. M., 1987, "Critical Speeds of Turbomachinery: Computer Predictions vs. Experimental Measurements—Part II: Effect of Tilt-Pad Bearings and Foundation Dynamics," Journal of Vibration, Acoustics, Stress, and Reliability in Design, *109*, pp. 8-14.

Wachel, J. C., 1986, "Design Audits," *Proceedings of the Fifteenth Turbomachinery Symposium*, Turbomachinery Laboratory, Texas A&M University, College Station, Texas, pp. 153-168.

ACKNOWLEDGEMENTS

The authors are indebted to the Elliott Company for permission to publish the work herein.